Journal of Materials Chemistry B

Accepted Manuscript

ROYAL SOCIETY OF CHEMISTRY

www.rsc.org/materialsB

Journal Name

ARTICLE

Polydopamine-induced nanocomposite Ag/CaP coatings on titania nanotubes surface forantibacterial andosteointegrationfunction†

Received 00th January 20xx,
Accepted 00th January 20xx

DOI: 10.1039/x0xx00000x

www.rsc.org/

Ming Li [a], Qian Liu[a], Zhaojun Jia [a], Xuchen Xu [a], Yuying Shi[a],Yan Cheng[a*], Yufeng Zheng[a,b]

The initial implant-associated infections and post aseptic loosening are the major obstacles for the clinical applications of titanium-based dental and orthopedic implants. To tackle with these issues, the implant surface is anticipated and engineered to possess combined osteointegration and antibacterial properties. Therefore, a mussel-inspired novel nano silver / calcium phosphate (CaP) composite coating was prepared on the anodized Ti, expecting its surface maintaining preferable biological performance and possessing long-term antibacterial ability. This approach involves three steps: (i) the anodic oxidation of Ti to enable it to have a TiO_2 nanotubular (TNT) surface structure,(ii) the self-polymerization of dopamine on TNT and the reduction of Ag and (iii) the modification of the Ag nanoparticles using polydopamine and further being immersed in SBF for the biomimetic mineralization of CaP. The surface morphology and microstructure of this novel coating was fully characterized. The Ag/CaP coatings displayed obvious antibacterial effects to S. aureus bacterial and relatively good *in vitro* cytocompatibility to MG63 cells. Compared with the pristine Ti, the cells cultured on the coated Ti showed enhanced ALP activities.

1. Introduction

Over the half past century, the use of biomaterials in the form of implants and medical devices is rising continuously with the population aging and advancements in the manufacture of synthetic biomaterials and surgical techniques. Titanium (Ti) and its alloys have been widely used for load-bearing hard tissue replacement including orthopedic and dental implants as well as fracture fixation hardware due to their excellent biocompatibility and outstanding mechanical properties. However, a major concern with these implants is the possibility of failure due to the lack of bone integration or the infections, particularly for the fixation of open-fractured bones and revision surgeries. It is reported that 0.5-3.0% primary and up to 8% revision implants have failed in total hip arthroplasty because of the bacterial infection which complicate tissue integration process [1].The present systemic antibiotic treatment raises concerns as systemic toxicity, low efficiency and need for hospitalization. In this context, the most promising measures to improve the success rates of the implant surgeries are modifications of the surface morphology and chemical composition of the medical devices to encourage the bone cells growth and inhibit the bacterial adhesion [2, 3].

Calcium phosphate (CaP) mineral is the main inorganic component of vertebrate bone and teeth, and it has been clinically successfully used as coatings on load-bearing metallic implants forboth dentistry and orthopedics due to its favorable interactions and integrations with bone tissue[4], especially for revision surgeries, but it was found that CaP-coated implants could also raise the surface affinity to bacteria[5, 6]. Combined with the above-mentioned risk of postsurgical infection, recently there is a great motivation to preparedual-functional composite coatings which can simultaneously stimulate tissue healing and reduce infection rate. The incorporation of antibacterial agents, such as antibiotics, silver, zinc and copper ions into the HA coating has important clinical values to improve the antibacterial activity of the medical implants [7-10]. Silver has been used as antibacterial agents over 6000 yearsin the form of ions, element, zeolite or nanoparticles for the treatment of burns, wounds and implant-associated infection (such as catheters, vascular grafts and endotracheal tubes) owing to its intrinsic potent andbroad antibacterial activity, less likely bacteria resistance, higher thermal stability, especially lower or lack of toxicity to humans [11-13]. Recently,the increase in antibiotic-resistant microorganisms has prompted resurgent interest in the use of silver as a potential antimicrobial agent for reducing bacterial adhesion and preventing biofilm formation[14-18].Compared with the silver-loaded polymer coatings, incorporating silver into bioactive ceramic HA coatings not only have the advantages of higher osseointegration ability and effective inhibition of local inflammatory reactions, but also can fulfill the mechanical requirement for load-bearing implants. Ag/CaP composite coating is one of the most promising dual function coatings for load-bearing implants, which has been prepared by serveral methods, such as

[a] Center for Biomedical Materials and Tissue Engineering, Academy for Advanced Interdisciplinary Studies, Peking University, Beijing 100871, People's Republic of China.
b Department of Materials Science and Engineering, College of Engineering, Peking University, Beijing 100871, People's Republic of China.
* Corresponding author email: chengyan@pku.edu.cn
† Electronic Supplementary Information (ESI) available: XRD analysis methods and results of the samples. See DOI: 10.1039/x0xx00000x

plasma spraying [7, 19-21], coprecipitation [20], magnetron co-sputtering [22], electrochemical deposition [23], plasma-based ion implantation and sputtering [24], sol-geltechnology[25, 26] ,slurry deposition [27], etc.

Inspired by catechol and amine functional groups of mussel adhesive proteins, polydopamine coating has attracted enormous interests in the last few years. By simply one-step immersion of substrates in a mild basic solution, dopamine could rapidly self-polymerize and form a tightly adhered polydopamine coating on virtually any materials surface and serve as a versatile secondary reaction platform [28].The fact that polydopamine has a close lattice match with hydroxyapatite and a strong binding ability to calcium and phosphate ions facilitating the biomimetic hydroxyapatite formation in simulated body fluid [29-33]. Furthermore, The metal-binding ability of catechols in polydopamine could contribute to the reduction of metal ions, such as Cu [28], Ag [34, 35], etc.

Recently, there is a great motivation to develop titania nanotubular arrays for high efficiency and controlled-release of drugs [36-39], such as antibacterial agents [40-42], growth factors [43], strontium [44], silver [45], zinc [46], bisphosphonate [47], even multi-drug [48] via tailoring the diameter and length of the nanotubes by simply varying the anodic parameters to promote osteointegration or reduce infection. Among them, Ag-containing/TiO_2 appears to be a very promising coating that greatly reduce the risk of bacterial adhesion and enhance the bactericidal effect. Roguska et al[49] prepared Ag/CaP coatins on anodized Ti substrate (TiO_2) using a combination of sputtering deposition technique (for Ag) and biomimetic mineralization method (for CaP) for biomedical applications. The Ag decorating process therein could be restricted by the sputtering equipment and the adhesion strength of the ontop CaP layer was too weak to be utilized for load-bearing applications[49]. Therefore a novel and convenient Ag/CaP coating preparation route should be developed and their *in vitro/in vivo* biocompatibility should be further investigated.

Herein a bio-inspired facile and simple method is presented for the generation of antibacterial and biointegrated Ag/CaP coatings on TiO_2 nanotubes. The advantage of using dopamine-induced method is thatthe polydopamine thin films can be strongly deposited onto practically any type of materials and three dimensional substrates with complex geometry. Compared with the above mentioned Ag/CaP coatings preparation techniques, the novelty of this research resides in the utilizing of dopamine as an adhesion agent (between coatings and substrate), a reductant (of Ag), a diffusion barrier (to decrease the release rate of Ag) and an inducer (to facilitate the biomineralization process) at the same time to enable the Ti surface with combined osteointegration and antibacterial properties, without the need of complicate equipments and reaction conditions. A hypothesis is proposed that local and sustained release of silver from biomimetic CaP-coated implants that can simultaneously promote tissue healing and reduce infection probabilities.

2. Materials and methods

2.1 Fabrication of TNT layer on Ti

Commercially pure titanium plate (99.5 % purity, 10 mm×10 mm×1 mm) purchased from Aldrich was used to form a titania nanotubular layer through anodization. The Ti plates were grounded by 400-, 1000- and 2000-grit SiC sandpapers; then successively and ultrasonically washed in acetone, 70 % alcohol and deionized water for 15 min, respectively. A two-electrode electrochemical anodization cell was used with stainless steel (50 mm×50 mm) as the cathode and Ti plate as the working electrode. The distance between the two electrodes was kept at 3 cm apart. All sampes were anodized in a glycerol/water (60:40) electrolyte containing 0.27 M ammonium fluorides at 15 V for 2 h. After anodization the samples were ultrasonically cleaned in deionized water and dried in nitrogen flow. The anodized samples were then heated at 500 ℃ for 2 h to enable the as-anodized amorphous TiO_2 nanotubes crystallize into the anatase structure, which were denoted as TNT.

2.2 Polydopamine-mediated deposition of Ag/CaP coatings on TNT

Fig. 1 shows the schematic diagram of polydopamine-induced nanocomposite Ag/CaP coatings on titania nanotubes surface, including dopamine self-polymerisation, silver reduction and CaP biomineralization. The TNT samples were soaked in 10 mL of a freshly prepared 2 mg/mL dopamine hydrochloride solution in 10 mM Tris buffer (pH=8.5) for 24 h at room temperature. The grafted polydopamine substrates were denoted as TNT-D. The TNT-D samples were incubated in 10 mL of 50 mM $AgNO_3$ solution at room temperature for 4 h (TNT-D-4A). Another polydopamine layer was formed by immersing in dopamine hydrochloride solution for 4 h to prevent Ag leaching and to induce biomineralization as well. Biomineralization was performed in simulated body fluid (1.5 SBF)[50]. The plates were soaked in 30 mL of 1.5 SBF solution and incubated at 37 °C for 1 d and 3 d. The SBF solution was changed every 24 h to provide sufficient ions for CaP deposition. When finished, the plates were removed from the solution, rinsed thoroughly with deionized water and dried in a vacuum oven. The plates were marked as Ag-D-xCaP (x=1, 3).

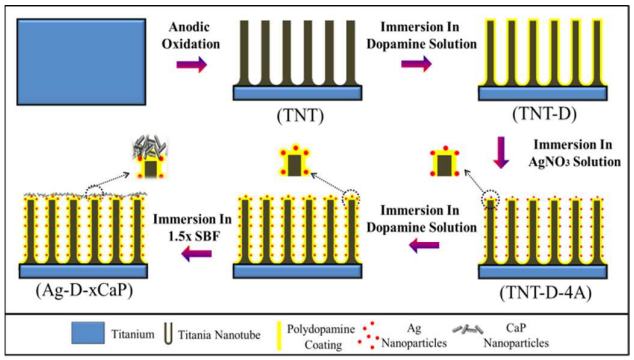

Fig.1 Illustration of anodization, dopamine polymerisation, silver reduction and CaP biomineralization on Ti

2.3 Surface morphology and microstructure characterization

Field emission scanning electron microscopy (FE-SEM, S-4800, Hitachi, Japan) was used to observe the surface topography of TNT layer and the Ag/CaP coatings, after being sputtering coated by an ultrathin gold as the conductive layer. The EDS (Bruke, Germany) and X-ray photoelectron spectroscopy (XPS, AXIS Ultra, Kratos Analytical Ltd.) were used to analysis the surface chemical composition. The crystal phase of the coating was identified by X-ray diffractometer (XRD, RigakuDmax, Japan) in the range of 10° - 80°. Fourier transform infrared spectroscopy (FT-IR, Nicolet 750, USA) was also used to examine phase composition and structural aspects of the CaP coatings before or after incubation in SBF solution. Finally, Contact angle measurements were carried out by the sessile-drop method (SL200B, Kino,USA) at room temperature. Two different liquids (deionized water and diiodomethane) were employed and the measurement was performed on 3 different spots on each substrate and the mean value of contact angles and surface energy were calculated.

2.4 Silver release

The Ag release of the samples was conducted by immersing the samples in freshly prepared phosphate buffered saline (PBS) (pH=7.4) in dark condition (one sample in 6 mL PBS) at 37 ^{o}Cfor a total of 14 d and the PBS solution was replaced every 24 h. The PBS solution containing released Ag ions was analyzed by inductively-coupled plasma atomic emission spectrometry (ICP-AES, Leeman, USA) to obtain the cumulative Ag release profiles.

2.5 Antibacterial rate assay

The antibacterial ability of the prepared samples was evaluated by using Staphylococcus aureus (S. aureus, ATCC 6538) cultivated in a Luria-Bertani (LB) medium. The bacteria suspension optical density (OD) was recorded by spectrophotometer at 600 nm after the two step activation with a value of 0.4-0.6. The samples were incubated in the bacteria suspension (one sample/500 μL) in LB at 37 ℃ for determined days. At the end of each incubation period, the specimens were gently rinsed thrice with PBS in order to eliminate the non-adherent bacteria. The viability of S. aureus adhered on the specimen was measured by Microbial Viability Assay Kit-WSK accordingly. The antibacterial rates of the specimen (Ra) were calculated based on the following formula: antibacterial rate equals (Ⅱ-Ⅰ) / Ⅰ×100%. Here, Ⅰ and Ⅱ is the average number of viable bacteria attached on the Ag-D-xCaP and TNT specimens respectively.

2.6 SEM observation of adhered bacteria

After 1 day incubation under the culturing condition mentioned above, the samples with S.aureus were rinsed in PBS for thrice and fixed in 2.5% glutaraldehyde for 2 h, followed by dehydration in gradient ethanol series each for 10 min and finally dried in air. The surfaces were then observed by SEM.

2.7 Fluorescent staining of adherent bacteria

Fluorescence staining was performed to study the viability and morphology of bacteria on the samples. The LB medium was changed very 24 h for 3 days. The culture medium was then removed and the samples were rinsed with PBS thoroughly, stained by a LIVE/DEAD Baclight bacterial viability kit (L7007, Invitrogen, USA) according to the manufacture's protocol. In this assay, the red-fluorescent nucleic acid staining agent propidium iodide, which only penetrates damaged cell membrane, was used to label dead bacterial cells. In contrast, the SYTO^{TM}-9 green-fluorescent nucleic acid staining agent, which can penetrate both intact and damaged cells membranes, was used to label all bacterial cell. The stained bacterial cells were examined under a Zeiss AIR-si laser scanning confocal microscope (Nikon, Japan). Images were captured using a 40× object lens under the same conditions.

2.8 Osteoblast-like cells culture

MG-63 osteoblast-like cells from human osteosarcoma (ATCC® CRL-1427TM, USA) were adopted to evaluate the cytotoxicity of the samples. MG-63 cells were cultured in Modified Eagle's Medium (MEM) with 10% fetal bovine serum (FBS), 100 U mL^{-1} penicillin and 100 mg/mL streptomycin (Invitrogen) at 37℃ in a humid atmosphere of 5 % CO_2. The medium was changed every 2 days until the cells became 90% confluence.

2.9 Osteoblast-like cell proliferation

The cytotoxicity of the samples toward MG-63 cells was evaluated by a cell counting kit-8 assay (CCK-8, Dojindo). All the samples were sterilized by ultraviolet-radiation for 2h on each side.500 μL cell suspensions were seeded onto the specimens in 24 well plates (one sample/one well) at a density of 4×10^4 cells/well. After 1 d, 3 d and 5 d incubation, 50 μL CCK-8 was added to each well for another 4 h incubation. Then 100 μL resulting medium from each well was transferred to 96 well plates using a pipette. In the control groups, MEM was used as negative control and MEM with 10 % dimethylsulfoxide (DMSO) as positive control. All samples were studied in triplicate. The measurement of the solution optical density (OD) was performed by a microplate reader (Bio-RAD 680) at 570 nm wavelength with a reference wavelength of 630 nm.

2.10 Immunofluorescence

MG-63 cells were cultured with specimens in 24 well plates for 3 days and the cells were washed with PBS and fixed with 4% (W/V) paraformaldehyde in PBS for 15 min at room temperature. The samples were then washed with PBS and permeabilizedby 0.1% (V/V) Triton X-100 (Sigma) for 3 min, followed by being incubated with 1% bovine serum albumin/PBS at 37 ℃ for 30 min to block nonspecific binding. Then the samples were treated with 5 μg/mL FITC-phalloidin (Molecular Probes, Eugene, OR) to stain MG-63 cells for 60 min. After being washed by PBS, samples were incubated for 5 min at room temperature with 5 μg/mL DAPI (Sigma-Aldrich). Then the samples were washed through PBS completely, and then the stained signals in the cells were observed by the fluorescent microscopy. Images were captured using a 40 × object lens under the same conditions.

2.11 Alkaline phosphatase activity

The alkaline phosphatase (ALP) activity was determined by using a test kit (Nanjing Jiancheng Bioengineering Institute, China) according to the assay protocol. A 1 mL cell suspension was seeded on each specimen at a density of 2×10^4 cells/mL in 24 well-plate. After being culture for 7 days, the supernatant was removed and 100 mL lysis solution (1 % TritonX-100) was added to each well for 1 h. 30 μL of the resulting MG-63 cell lysates was transferred to a new 96-well plate, and cultivated with 50 μL carbonated buffer solution (pH=10) and 50 μL substrate solution (4-amino-antipyrine) at 37 ℃ for 15 min. Then 150 μL chromogenic agent (potassium ferricyanide) was added into the mixed solution. A spectrophotometer (Elx-800, bio-Tek instruments) was utilized to measure the OD values at 520 nm.

2.12 Statistical analysis

The data were expressed as means±standard deviations. Each experiment was repeated three times. A one-way ANOVA test was utilized to determine the level of significance, $p < 0.01$ was regarded to be significantly different.

3. Results and Discussions

3.1 Surface morphology and composition of the coatings

In order to obtain a strong adhesive polydopamine-based coating with well reduced and distributed Ag nanoparticles and to enable this coating as a better platform for CaP nucleation and deposition, the optimized times of polymerization of dopamine and reduction of Ag on TNT were studied. The TNT surfaces were coated by polymerized dopamine after 4 h and 24 h reaction, respectively. The dopamine coated TNT surfaces still maintained well orderly nanotubular structure for all the samples. As shown in Fig.2, after being soaked in dopamine for 4 h and then immersed in $AgNO_3$ for 10 min to 24 h, the distribution and particle size of the Ag nanoparticles reduced by the grafted polydpamine coatings displayed no significantly differences. When dopamine polymerized on TNT for 24 h, the deposited Ag nanoparticles became larger and larger with the prolonged reduction time. Ag clusters or aggregates could be observed on the 24 h polydopamine coated TNT. Therefore, TNT samples were subjected to 24 h immersion in dopamine and 4 h in $AgNO_3$, before being further coated by biomimetic mineralization.

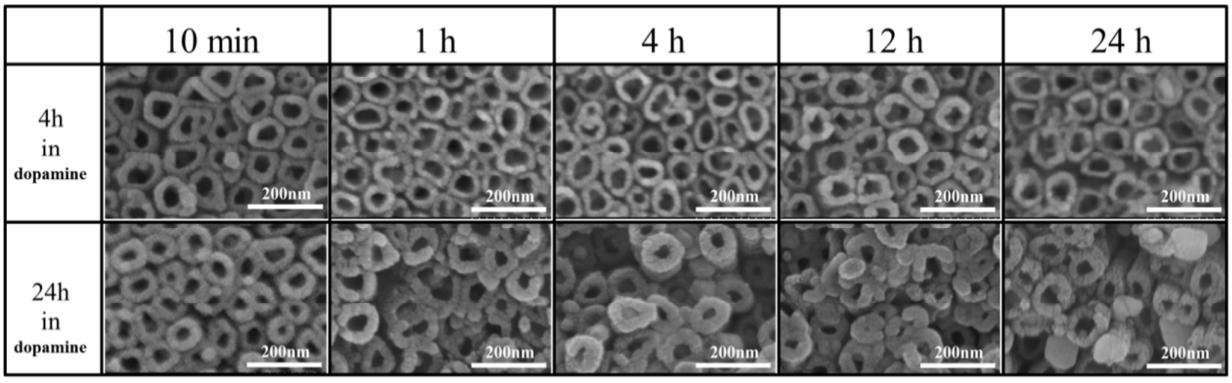

Fig.2 The SEM surface morphology of the Ag nanoparticles decorated poly-dopamine coatings on TNT

Journal Name

ARTICLE

The motivation of fabricating dopamine mediated Ag/CaP coatings on TNT surfaces resides in that the intermediate TiO_2 nanotubular layers obtained from the anodic oxidation was supposed to (1) increase the binding strength of the resulting coatings on top, as the anodized Ti could produce an intermediate oxidelayer rich in -OH or Ti-O-, which would induce strong electrostatic interactions or hydrogen-bondinteraction with the top coating materials (eg. hydroxyapatite deposition and dopamine polymerization) [51], (2) be functionalized as carriers for loading drug/nanoparticles with increased loading capacity and long-term sustained release due to their increased surface area and novel nano-scale morphology[52], and (3) enhance the osteointegration by providing a favorable circumstance for the growth and maintenance of bone cells[53], (4) antibacterial property as suggested that the nano-structured titanium with nanotubes in diameters of 80 nm displayed the most robust antimicrobial effect and (5) increase of corrosion resistant properties of the titanium substrate[54].

TNT-D-4A was then functionalized by being immersed in 1.5 SBF for 1 d and 3 d, respectively; the SEM and mapping mode EDS images of the coatings were shown in Fig. 3. The Ag-D-xCaP (x=1, 3) samples showed obvious different morphology which indicated that the immersion time of the samples in SBF significantly affect the structures of samples. For the Ag-D-1CaP coatings, the nanotubular surfaces were covered by a dense Ag/CaP composite coatings with uniformly decorated Ag particles and CaP aggregates. After being soaked in SBF for 3 d, these aggregates transformed into large CaP clusters with porous structures.

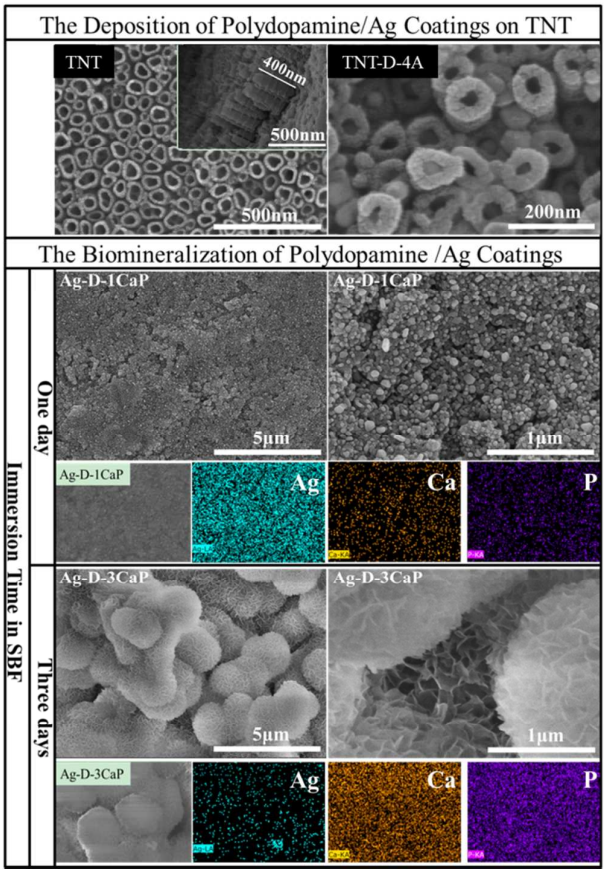

Fig.3 SEM and EDS images of the biomineralizatin of polydopamine mediated Ag coatings on TNT surface after 1 d and 3 d immersion in 1.5 SBF, respectively

Table 1. Surface chemical composition of samples obtained from XPS analysis

Samples	Atomic percentage%						
	Ti	O	C	Ag	N	Ca	P
TNT	23.46	61.53	15.01	-	-	-	-
TNT-D	0.11	19.41	72.47	-	8.01	-	-
TNT-D-4A	0.66	18.99	65.97	4.88	9.50	-	-
Ag-D-1CaP	0.57	20.42	66.22	4.12	5.53	1.89	1.25
Ag-D-3CaP	0	43.80	28.60	0.60	1.94	14.10	10.95

The resulting coatings were also subjected to XPS analysis and the detected N indicated the successful polymerization and deposition of dopamine on the TNT surface. Fig.4a shows the XPS spectra of dopamine mediated deposition of Ag and CaP coatings on TNT surface. Table 1 displays chemical composition of dopamine mediated Ag and CaP coatings on TNT surface by XPS. Compared with TNT-D-4A, the Ti, Ag and N contents were decreased after 3 d biomineralization, with significantly increase in Ca and P contents; and the decrease of N from 9.5 at. % to 1.94 at. % indicated the almost fully coverage of the polydopamine layer by the CaP deposites. Sample of Ag-D-3CaP with CaP as outermost layer possesses the highest of Ca, P contents of 14.10 at.% and 10.95 at.% respectively.Therefore, the combined qualitative (mapping mode EDS images) and quantitative (surface chemical composition in Table 1) results suggested that after being immersed in 1.5 SBF for 3 d, the Ag-D-3CaP samples were fully deposited by thick CaP layers.

The Ca/P ratio for the calcium phosphate deposits obtained on Ag-D-3CaP was close to the stoichiometric ratio of hydroxyapatite (Ca/P=1.67, $Ca_{10}(PO_4)_6(OH)_2$)) indicating that the polydopamine layers provided sufficient catechol groups available for CaP nucleation.

To further investigate the chemical structure and molecule interaction, high resolution spectra of O 1s, Ca 2p, P 2p and Ag 1s characterized on Ag-D-3CaP samples are shown in Fig.4b. The O 1s binding energy at 530.1 eV correspond to typical binding energies for TiO_2 [55, 56]. The band energy of O1s spectrum at 533.8 eV could come from the phosphate bonds in HA. Ag element is observed at 374.25 eV and 368.25 eV which attributed to Ag $3d_{3/2}$ and Ag $3d_{5/2}$ of metallic Ag^0, respectively, suggesting the successful reduction of Ag^+ to Ag. The P 2p band consists of two peaks at E_{bind}=133.5 eV and 134.3 eV while Ca 2p band consists of two peaks at E_{bind}=347.72 eV and 351.26 eV.

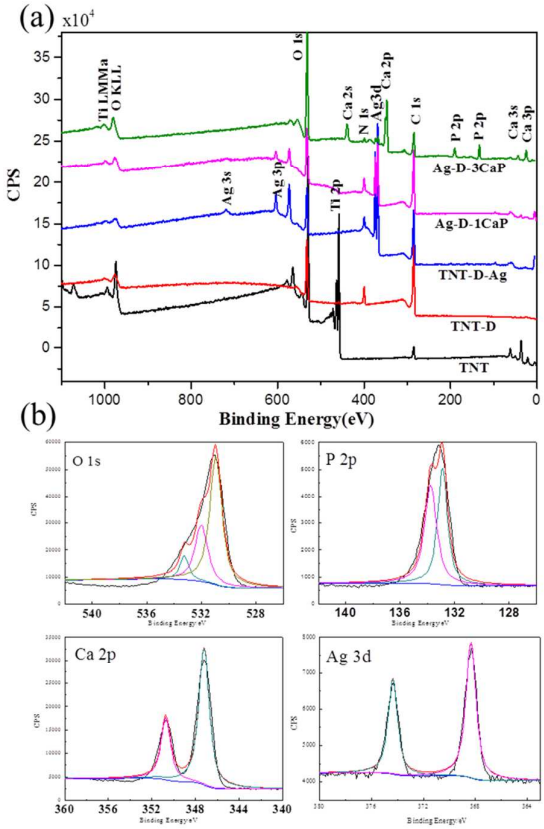

Fig.4 The XPS survey spectra of samples (a) and the high-resolution XPS spectra (b) of O 1s, Ca 2p, P 2p and Ag 3d of the of Ag-D-3CaP coatings

The FT-IR of the functionalized samples was shown in Fig. 5. The spectrum of Ag-D-3CaP is dominated by the PO_4^{3-} stretching vibration in the 1000-1100 cm^{-1} range. The bands detected at 1648 cm^{-1} were assigned to C-N bending vibrations and 1230 cm^{-1} for N-H vibration implying the deposition and formation of polydopamine on the TNT surface. The bands at 1460 cm^{-1}, 1420 cm^{-1} (C-O) and 1584.6 cm^{-1} were contributed to the CO_3^{2-} adsorption, especially for the 1584.6 cm^{-1} which originated from the substitute for OH^- during the deposition of Ca/P. As the biomimetic mineralization process was conducted in unconfined atmospheric environment, the detected carbonate groups were originated from the absorption of the CO_2, which resulted in the formaion of A-type carbonated hydroxyapatite (partially substitution of hydroxide ions by carbonate ions)[57]. Characteristic peak at 874.2 cm^{-1} indicates the presence of HPO_4^{2-}[58]. Besides, the broad band in the 3000-3500 cm^{-1} range and the band at about 1650 cm^{-1}were attributable to vibrational modes of absorbed water. Ag-D-3CaP sample occupies obviously higher peak intensity of PO_4^{3-} than Ag-D-1CaP indicating higher content of Ca and P, which is identical to EDS results. The XRD patterns in Fig.S1 suggested that the deposited CaP mainly consisted of hydroxyapatite.

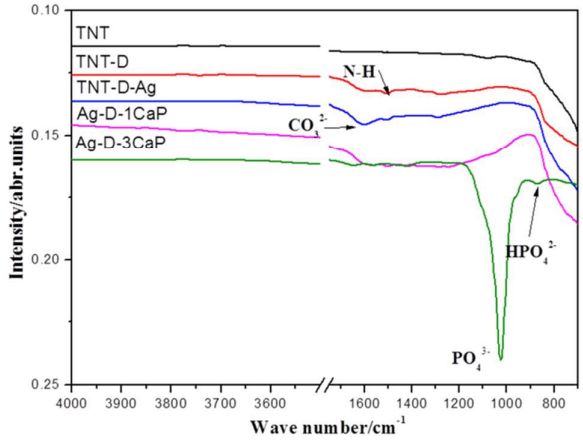

Fig.5 The FT-IR spectra of the samples

The presence of distinct phosphate bands in the FT-IR spectrumshows that the polydopamine modified TNT surface is a favorable substrate for apatite nucleation and deposition.

Further characterization of the coating wettability is performed through contact angles analysis. The contact angles and the calculated surface free energy of Ti, TNT and polydopamine treated samples are shown in Table 2. After anodization, the contact angle of Ti was decreased significantly from 60.04° to 4.09°. The polydopamine modified surface was confirmed to be more hydrophilic than that of titanium surface. While the hydrophilicity of polydopamine mediated Ag samples TNT-D-4A are stronger than that of the TNT-D samples. The Ag-D-1CaP sample exhibit excellent hydrophilicity and higher surface energy. Ag particles facilitate the apatite nucleation [59]. Increased surface free energy were suggested to be benefit for the cell adhesion and viability [60, 61].

Table 2. Contact angles and values of surface free energy of the samples

Samples	Contact angle(deg)		Surface free energy(mJ/m^2)		
	DI water	Diiodomethane	D.F.[a]	P.F.[a]	S.F.E.[a]
Ti	60.04±3.85	35.40±1.40	41.84	11.65	53.49
TNT	4.09±1.48	3.71±1.38	50.69	30.53	81.23
TNT-D	21.07±2.88	13.27±2.66	49.45	27.62	77.07
TNT-D-4A	12.83±1.13	7.6±1.81	50.35	29.45	79.81
Ag-D-1CaP	11.96±0.50	9.77±0.97	50.06	29.78	79.84

[a]Note: D.F=dispersive force, P.F.=polar foce, S.F.E.=surface free energy

The results above suggested that longer immersion in SBF could result in thicker Ca/P deposits. This project was designed to endow

the Ti substrate with combined antibacterial and osteointegrate abilities. The coating consisted of four layers with a sequence of Ti-D1-Ag-D2-Ca/P, where D represents polydopamine, and in which the D1 acted as adhesion agent (to bind the coatings and the substrate) and reductant (to obtain Ag nanoparticles) and D2 functionalized as a diffusion barrier (to decrease the release rate of Ag so as to reduce its cytotoxicity) and an inducer (to facilitate the biomineralization process).Ag has been widely acknowledged as an effective antimicrobial substance, but also showing cytotoxicity to some mammalian cell. Therefore, it is of great significance to mediate the Ag release rate to ensure its initial bactericidaleffect and maintain its post cell biocompatibility. Ag was reduced and anchored by D1 on the anodized Ti and being further coated by D2 and Ca/P. The deposited Ca/P was supposed to increase the biocompatibility of the Ti-D1-Ag. Combined with the observation of surface morphology and the characterization of the surface composition, it seems to fall into a dilemma that longer immersion in SBF could resulting in thicker Ca/P but lower content of Ag. One possible explanation for this is that the biomineralization process of Ti-D1-Ag-D2 was also accompanied by the dissolution of Ag. It was reported that the infection of the implant surgery usually occurred within 4 hours of the post operation and the prosthetic infections was initiated by the adhesion of the bacteria. As a result, it is expected that the composite coating could release higher content of Ag when the sample was implanted, and then its adverse effects on the adjacent tissues could be alleviated and compensated by the Ca/P minerals. Therefore, Ag-D-1CaP was selected for the following Ag release and in vitro cytotoxicity analysis in order to shed light on its possible application in bone-related areas.

3.2 Ag ion release

Fig. 5 shows the cumulative Ag release vs. time profiles from the Ag-D-1CaP samples in 6 mL PBS as described previous. The precipitated CaP layer on Ag was expected to decrease the dissolve rate of Ag ions, therefore prolonging the releasing time of this bacteriocidal substance and enhancing the biocompatibility of the coatings. Initially, the Ag releasing rate was relatively faster. After being immersed in PBS for 3 d , the Ag releasing rate was decreased. From Table 1, Ag-D-1CaP samples occupied 4.12 at.% Ag, which indicated the actively metallization of Ag through the interaction between polydopamine and silver nitrate. Such results indicated the long-term antibacterial activity could be achieved from Ag-D-1CaP samples. The amounts of released Ag diminished gradually with immersion time. Silver toxicity was reported to occur at serum levels as low as 0.3 ug/mL and manifests as argyria, leukopenia, and alterations in renal, hepatic, and neural tissues[62].By the end of this immersion test, the Ag concentration is around 2 μg/mL and higher than 0.3 μg/mL. The toxicity of Ag nanoparticles is closely related to the release of Ag ions [63]. The Ag concentration in this immersion study was calculated by accumulative Ag release amount in PBS, and its cytotoxicity might be potentially alleviated by the dillution of the adjacent biological fluid when putting the samples into clinical applications.Besides, in biological media, the dissolution of Ag nanoparticles is strongly influenced by sulfur ions, chloride ions, dissolved oxygen and other biological macromolecules (DNA, protein) that have strong affinityto Ag, as well as the pH and the lightening conditions[63]. Therefore more researches should be conducted to clarify this issue.

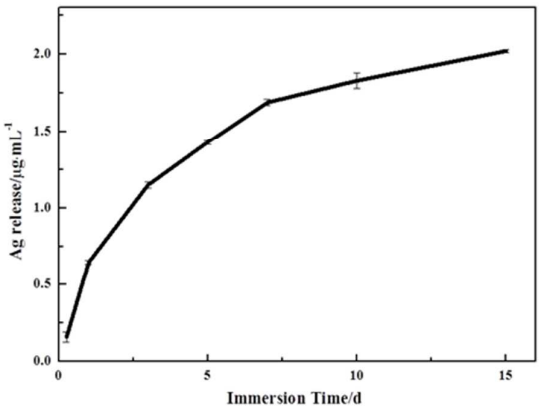

Fig.6 The cumulative Ag release vs. time profiles from the Ag-D-1CaP samples

3.3 Antibacterial properties

SEM is performed to investigate the morphology of S. aureus bacterial on the polydopamine mediated Ag and CaP samples, with the untreated Ti as control group. As it is shown in Fig. 7, the S. aureus cells aggregated together on Ti surface forming into large culsters. These bacteria were less aggregated and displayed round and intact shape on the TNT surface. The anatase TiO2 photocatalysis promoted peroxidation of the polyunsaturated phospholipids component of the lipid membrane and induced major disorder in the bacteria [64]. Meanwhile, obviously less and dispersive cells were observed on Ag-D-1CaP samples, indicating that incorporation of Ag nanoparticles can significantly enhance the antibacterial activity of the TNT coating.

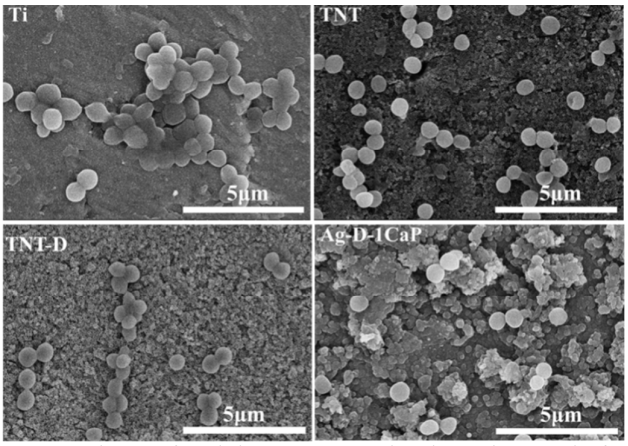

Fig.7 SEM images of Staphylococcus aureus cultured on various samples for 1 d

To further evaluate the antibacterial activity of the TNT-D and dopamine mediated Ag and CaP samples, their antibacterial rates

against S. aureus bacteria for adherent bacteria on the specimens for 3 days and 7 days were evaluated and the results are shown in Fig. 8. Compared with the TNT-D samples, the Ag-D-1CaP samples possessed higher antibacterial efficiency since the antibacterial rate of S. aureus seeded on Ag-D-1CaP coating reached at 72% after 7 days co-culture. For the Ag-D-1CaP samples, the fully polymerization of dopamine could reduce more Ag metallic particles from Ag+ in the solution as shown in Table 1. Moreover, the CaP coatings formed through the polydopamine functionalization are porous. The leaked Ag ions through the CaP minerals provide the ability to kill the attached bacteria.

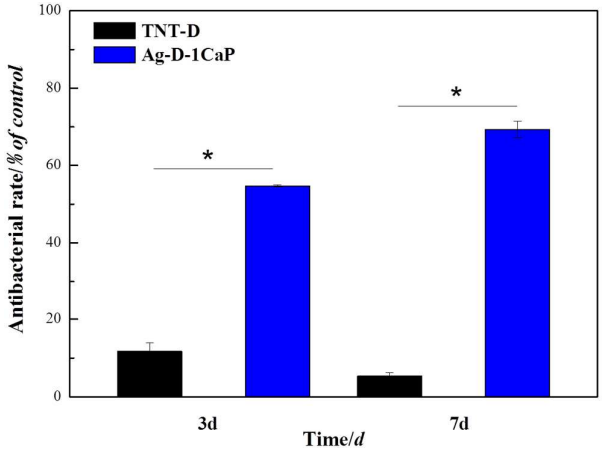

Fig.8 The antibacterial rates of the samples against S. aureus bacteria after co-culturing for 3 d and 7 d.* represents $p < 0.01$

3.4 Fluorescence staining assay

The ability of the Ag-D-1CaP samples to prevent viable bacteria colonization was also verified by fluorescence staining as shown in Fig. 9. TNT samples were used as control group since all the samples were prepared on the TNTs surface. The samples were stained using a LIVE/DEAD Baclight bacterial viability kit (L7007, Invitrogen, USA). The red fluorescent was used to label dead bacterial cells while the green fluorescent was used to label all the live bacterial cells. After 3 days of bacteria invasion with fresh LB medium changed every 24 h, the deadcells were washed away and therefore the red-stained cells could not observed on all the samples. Meanwhile, there were relatively large amounts of viable bacteria on TNT. There also existed several bacterial agglomerations on the surface, which might further develop into biofilm. Once the biofilm was formed on the interface, severe infection could occur. The polydopamine coated TNT showed homogeneous adhered bacterial equally to the TNT surface. However, all the bacteria were separated without agglomerations. And the polydopamine coatings were reported to have the antibacterial ability to some extent [65]. In comparison, the Ag-D-1CaP samples displayed good antibacterial ability towards the S. aureus. Particularly, nearly no viable bacteria could be seen on the Ag-D-1CaP samples. These results are identical with the antibacterial rate.

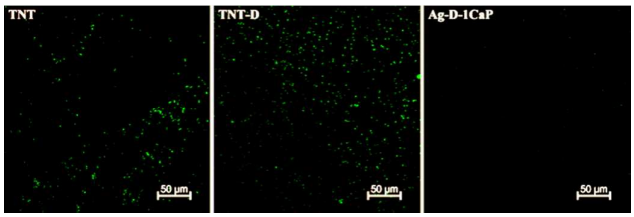

Fig.9 Live/dead cells staining on TNT, TNT-D, Ag-D-1CaP samples after 3 d incubation with S. aureus bacteria

3.5 The osteoblast-like cell viability

The proliferation and vitality of MG-63 cells cultured on the TNT, TNT-D, and Ag-D-1CaP samples for 1 d, 3 d and 5 d were determined by CCK-8 assay, and the results are shown in Fig. 10. Compared with TNT samples, the TNT-D samples showed slightly higher vitality which was consistent with the previous studies[28]. When the culture time prolonged to 5 d, Ag-D-1CaP samples exhibited slightly stronger suppression on cell viability than that of TNT and polydopamine treated samples. Studies performed by Ku et al.[66] suggested that polydopamine functionalized surfaces could support the normal growth of mammalian cells without cytotoxicity. The reason underlying the observed attenuation of the in vivo toxicity is supposed to be that the critical surface tension of polydopamine is 35-40 dyne/cm, which falls into a suitable range for cell adhesion, minimizing structural changes in the surface-adsorbed proteins[67, 68].

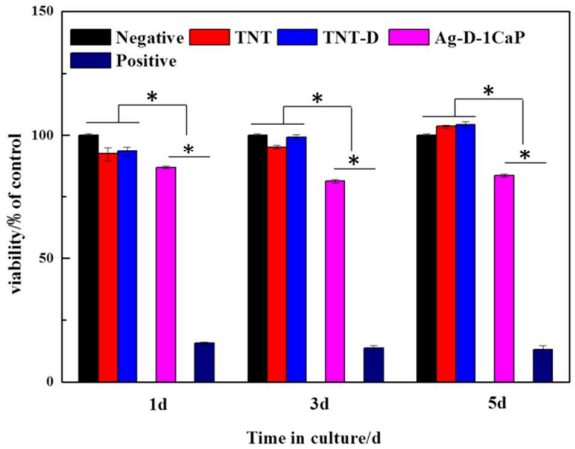

Fig.10 Viability of MG-63 cell cultured on TNT, TNT-D, Ag-D-1CaP samples for 1 d, 3 d and 5 d. * represents $p < 0.01$

It seems to be a dilemma that higher amount of Ag can result in higher antibacterial rate, but also lead to higher cytotoxicity. Therefore, more researches should be undertaken to optimize the Ag dose or release rate to enable the composite coating with combined well cytocompatibility and desired antibacterial properties.

3.6 Cytoskeletal observation

To examine the influence of the Ag-loaded samples on the cellular morphology, the fluorescent staining of MG-63 cells were conducted. Fig.11 displays the morphologies of MG-63 cultured on different functionalized samples. Cell numbers for polydopamine coated samples TNT-D were not enhanced compared with those of TNT samples. However, the Ag-D-1CaP samples showed less attached MG-63 cells but still spread with visible mature F-actin intracellular stress fibers. The well spread cellular pseudopods indicated that Ag-D-1CaP samples exhibited relatively good in vitro cytocompatibility.

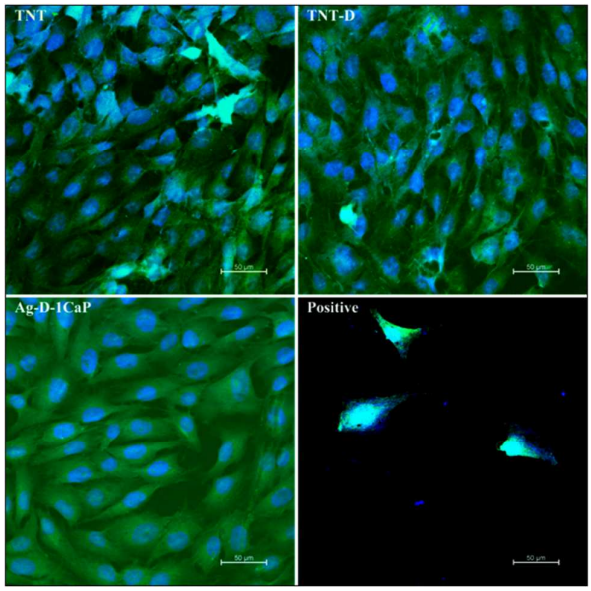

Fig.11 Adhesion morphology and actin cytoskeletal organization (green, labeled with FITC-phalloidin, counterstained with DAPI for nuclei inblue) of MG-63 cells after incubation with TNT, TNT-D, Ag-D-1CaP samples for 3 d

3.7 Alkaline phosphatase activity

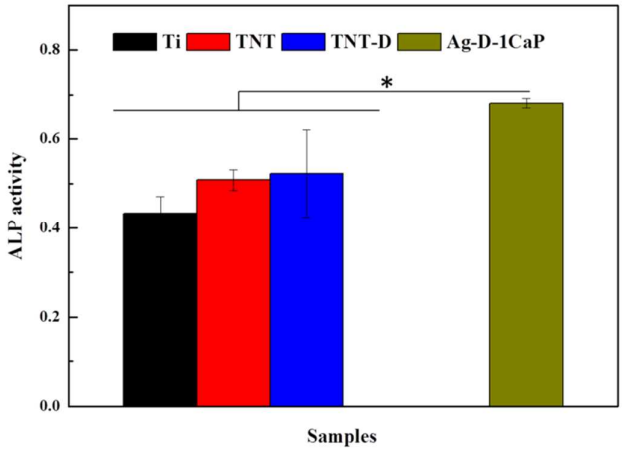

Fig.12 The ALP activity of MG-63 cells cultured on the TNT, TNT-D, Ag-D-1CaP surfaces for 7 d. * represents $p < 0.01$

ALP activity of the cells after 7 d culturing with the samples is shown in Fig. 12. The TNT and TNT-D samples showed slightly higher ALP activity than that of the pure Ti. The highest ALP activity was observed from the Ag-D-1CaP, which demonstrated that the chemical composition and morphology of the outermost layer had a great influence on the biocompatibility of the samples.

4. Conclusions

In this study, a novel composite coating with combined antibacterial and osteointegrated properties was successfully fabricated on the anodized Ti substrate through a mussel-inspired facile and simple method. Within this coating, dopamine was employed by self-polymerization on TiO_2 nanotubular surface and functionalized as an adhesion agent of the coatings, a reductant and diffusion barrier of Ag and an inducer for biomineralization. The resulting samples (Ag-D-1CaP) showed obvious antibacterial ability while maintain good biological performance. It could prevent the initial and intermediate-stage infection after operation and perhaps relatively long term infection. The ontop CaP coatings could alleviate the adverse influences of Ag on the proliferation of the osteoblasts and achieve a better biological performance through the synergistic effects of polydopamine and Ag/CaP. The prepared samples are very promising for biomedical implant applications due to their potential to prevent implant associated infection and promote the osteointegration.

5.Acknowledgements

This work is jointly supported by the Project of Scientific and Technical Plan of Beijing (No. Z141100002814008), National Natural Science Foundation of China (No. 31370954) and State Key Laboratory of Bioelectronics Open Research Fund of China (Chien-Shiung Wu Laboratory).

Notes and references

1. A. G. Gristina, *Science*, 1987, **237**, 1588-1595.
2. H. Schliephake and D. Scharnweber, *J Mater Chem*, 2008, **18**, 2404-2414.
3. A. Montali, *Injury*, 2006, **37**, 81-86.
4. R. A. Surmenev, M. A. Surmeneva and A. A. Ivanova, *Acta Biomater*, 2014, **10**, 557-579.
5. C. J. M. Oosterbos, H. C. Vogely, M. W. Nijhof, A. Fleer, A. J. Verbout, A. J. Tonino and W. J. A. Dhert, *J BiomedMater Res*, 2002, **60**, 339-347.
6. P. A. Norowski and J. D. Bumgardner, *J Biomed Mater Res B*, 2009, **88B**, 530-543.
7. M. Roy, G. A. Fielding, H. Beyenal, A. Bandyopadhyay and S. Bose, *Acs Appl Mater Inter*, 2012, **4**, 1341-1349.
8. M. Stigter, K. de Groot and P. Layrolle, *Biomaterials*, 2002, **23**, 4143-4153.
9. V. Alt, A. Bitschnau, J. Osterling, A. Sewing, C. Meyer, R. Kraus, S. A. Meissner, S. Wenisch, E. Domann and R. Schnettler, *Biomaterials*, 2006, **27**, 4627-4634.

10. S. Radin, J. T. Campbell, P. Ducheyne and J. M. Cuckler, *Biomaterials*, 1997, **18**, 777-782.
11. J. Hardes, H. Ahrens, C. Gebert, A. Streitbuerger, H. Buerger, M. Erren, A. Gunsel, C. Wedemeyer, G. Saxler, W. Winkelmann and G. Gosheger, *Biomaterials*, 2007, **28**, 2869-2875.
12. B. S. Atiyeh, M. Costagliola, S. N. Hayek and S. A. Dibo, *Burns*, 2007, **33**, 139-148.
13. M. Bosetti, A. Masse, E. Tobin and M. Cannas, *Biomaterials*, 2002, **23**, 887-892.
14. J. W. Alexander, *Surg Infect*, 2009, **10**, 289-292.
15. S. Chernousova and M. Epple, *Angew Chem Int Edit*, 2013, **52**, 1636-1653.
16. K. N. J. Stevens, S. Croes, R. S. Boersma, E. E. Stobberingh, C. van der Marel, F. H. van der Veen, M. L. W. Knetsch and L. H. Koole, *Biomaterials*, 2011, **32**, 1264-1269.
17. K. Chaloupka, Y. Malam and A. M. Seifalian, *Trends Biotechnol*, 2010, **28**, 580-588.
18. D. R. Monteiro, L. F. Gorup, A. S. Takamiya, A. C. Ruvollo, E. R. Camargo and D. B. Barbosa, *Int J Antimicrob Ag*, 2009, **34**, 103-110.
19. L. Song, Y. F. Xiao, L. Gan, Y. Wu, F. Wu and Z. W. Gu, *Surf Coat Tech*, 2012, **206**, 2986-2990.
20. Y. K. Chen, X. B. Zheng, Y. T. Xie, H. Ji, C. X. Ding, H. W. Li and K. R. Dai, *Surf Coat Tech*, 2010, **205**, 1892-1896.
21. Y. K. Chen, X. B. Zheng, Y. T. Xie, C. X. Ding, H. J. Ruan and C. Y. Fan, *J Mater Sci-Mater M*, 2008, **19**, 3603-3609.
22. W. Chen, Y. Liu, H. S. Courtney, M. Bettenga, C. M. Agrawal, J. D. Bumgardner and J. L. Ong, *Biomaterials*, 2006, **27**, 5512-5517.
23. X. Lu, B. L. Zhang, Y. B. Wang, X. L. Zhou, J. Weng, S. X. Qu, B. Feng, F. Watari, Y. H. Ding and Y. Leng, *J R Soc Interface*, 2011, **8**, 529-539.
24. N. A. Trujillo, R. A. Oldinski, H. Y. Ma, J. D. Bryers, J. D. Williams and K. C. Popat, *Mat Sci Eng C-Mater*, 2012, **32**, 2135-2144.
25. W. Chen, S. Oh, A. P. Ong, N. Oh, Y. Liu, H. S. Courtney, M. Appleford and J. L. Ong, *J Biomed Mater Res A*, 2007, **82A**, 899-906.
26. R. J. Chung, M. F. Hsieh, C. W. Huang, L. H. Perng, H. W. Wen and T. S. Chin, *J Biomed Mater Res B*, 2006, **76B**, 169-178.
27. J. J. Blaker, S. N. Nazhat and A. R. Boccaccini, *Biomaterials*, 2004, **25**, 1319-1329.
28. H. Lee, S. M. Dellatore, W. M. Miller and P. B. Messersmith, *Science*, 2007, **318**, 426-430.
29. J. Ryu, S. H. Ku, M. Lee and C. B. Park, *Soft Matter*, 2011, **7**, 7201-7206.
30. J. Ryu, S. H. Ku, H. Lee and C. B. Park, *Adv Funct Mater*, 2010, **20**, 2132-2139.
31. M. Lee, S. H. Ku, J. Ryu and C. B. Park, *J Mater Chem*, 2010, **20**, 8848-8853.
32. C. T. Wu, P. P. Han, X. G. Liu, M. C. Xu, T. Tian, J. Chang and Y. Xiao, *Acta Biomater*, 2014, **10**, 428-438.
33. Z. G. Liu, S. X. Qu, X. T. Zheng, X. Xiong, R. Fu, K. Y. Tang, Z. D. Zhong and J. Weng, *Mat Sci Eng C-Mater*, 2014, **44**, 44-51.
34. D. E. Fullenkamp, J. G. Rivera, Y. K. Gong, K. H. A. Lau, L. H. He, R. Varshney and P. B. Messersmith, *Biomaterials*, 2012, **33**, 3783-3791.
35. T. S. Sileika, H. D. Kim, P. Maniak and P. B. Messersmith, *Acs Appl Mater Inter*, 2011, **3**, 4602-4610.
36. K. C. Popat, M. Eltgroth, T. J. La Tempa, C. A. Grimes and T. A. Desai, *Small*, 2007, **3**, 1878-1881.
37. P. Roy, S. Berger and P. Schmuki, *Angew Chem Int Edit*, 2011, **50**, 2904-2939.
38. Y. Y. Song, F. Schmidt-Stein, S. Bauer and P. Schmuki, *J Am Chem Soc*, 2009, **131**, 4230-+.
39. D. Losic and S. Simovic, *Expert Opin Drug Del*, 2009, **6**, 1363-1381.
40. M. Kazemzadeh-Narbat, B. F. L. Lai, C. F. Ding, J. N. Kizhakkedathu, R. E. W. Hancock and R. Z. Wang, *Biomaterials*, 2013, **34**, 5969-5977.
41. K. C. Popat, M. Eltgroth, T. J. LaTempa, C. A. Grimes and T. A. Desai, *Biomaterials*, 2007, **28**, 4880-4888.
42. L. L. Peng, A. D. Mendelsohn, T. J. LaTempa, S. Yoriya, C. A. Grimes and T. A. Desai, *Nano Lett*, 2009, **9**, 1932-1936.
43. K. S. Brammer, C. J. Frandsen and S. Jin, *Trends Biotechnol*, 2012, **30**, 315-322.
44. L. Z. Zhao, H. R. Wang, K. F. Huo, X. M. Zhang, W. Wang, Y. M. Zhang, Z. F. Wu and P. K. Chu, *Biomaterials*, 2013, **34**, 19-29.
45. F. Cui, J. Li, A. Ding, C. Zhao, L. Wang, X. Wang, S. Li, Y. Bao, X. Li, D. Feng, L. Kong and H. Wang, *TAG. Theor Appl Genet*, 2011, **122**, 1517-1536.
46. K. F. Huo, X. M. Zhang, H. R. Wang, L. Z. Zhao, X. Y. Liu and P. K. Chu, *Biomaterials*, 2013, **34**, 3467-3478.
47. S. H. Moon, S. J. Lee, I. S. Park, M. H. Lee, Y. J. Soh, T. S. Bae and H. S. Kim, *J Biomed Mater Res B*, 2012, **100B**, 2053-2059.
48. M. S. Aw, J. Addai-Mensah and D. Losic, *Chem Commun*, 2012, **48**, 3348-3350.
49. A. Roguska, M. Pisarek, M. Andrzejczuk, M. Lewandowska, K. J. Kurzydlowski and M. Janik-Czachor, *J Biomed Mater Res A*, 2012, **100A**, 1954-1962.
50. T. Kokubo and H. Takadama, *Biomaterials*, 2006, **27**, 2907-2915.
51. Y. Q. Wang, J. Tao, L. Wang, P. T. He and T. Wang, *T Nonferr Metal Soc*, 2008, **18**, 631-635.
52. C. Moseke, F. Hage, E. Vorndran and U. Gbureck, *Appl Surf Sci*, 2012, **258**, 5399-5404.
53. K. C. Popat, L. Leoni, C. A. Grimes and T. A. Desai, *Biomaterials*, 2007, **28**, 3188-3197.
54. I. Milosev, D. Blejan, S. Varvara and L. M. Muresan, *J Appl Electrochem*, 2013, **43**, 645-658.
55. L. Zhao, H. Wang, K. Huo, L. Cui, W. Zhang, H. Ni, Y. Zhang, Z. Wu and P. K. Chu, *Biomaterials*, 2011, **32**, 5706-5716.
56. S. Sobieszczyk, *Adv Mater Sci*, 2009, **9**, 25-41.
57. J. P. Lafon, E. Champion and D. Bernache-Assollant, *J Eur Ceram Soc*, 2008, **28**, 139-147.
58. S. Koutsopoulos, *J. Biomed. Mater. Res. Part A*, 2002, **62**, 600-612.
59. J. S. Lee and W. L. Murphy, *Adv Mater*, 2013, **25**, 1173-1179.
60. H. J. R. Marc Long, *Biomaterials* 1998, **19**, 1621-1639.
61. M. Geetha, A. K. Singh, R. Asokamani and A. K. Gogia, *Prog Mater Sci*, 2009, **54**, 397-425.
62. M. A. Nandkumar, M. Ranjit, S. P. Kumar, P. Hari, P. Ramesh and K. Sreenivasan, *Trends Biomater Artif Organs*, 2010, **24**, 156-164.

63. D. McShan, P. C. Ray and H. T. Yu, *J Food Drug Anal*, 2014, **22**, 116-127.
64. L. Zhao, P. K. Chu, Y. Zhang and Z. Wu, *J Biomed Mater Res B,* 2009, **91B**, 470-480.
65. M. Sureshkumar, D. Y. Siswanto, Y. C. Chen, C. K. Lee and M. J. Wang, *J Polym Sci Pol Phys*, 2013, **51**, 303-310.
66. S. H. Ku, J. S. Lee and C. B. Park, *Langmuir*, 2010, **26**, 15104-15108.
67. S. H. Ku, J. Ryu, S. K. Hong, H. Lee and C. B. Park, *Biomaterials*, 2010, **31**, 2535-2541.
68. C. Ozcan and N. Hasirci, *J Biomat Sci-Polym E*, 2007, **18**, 759-773.

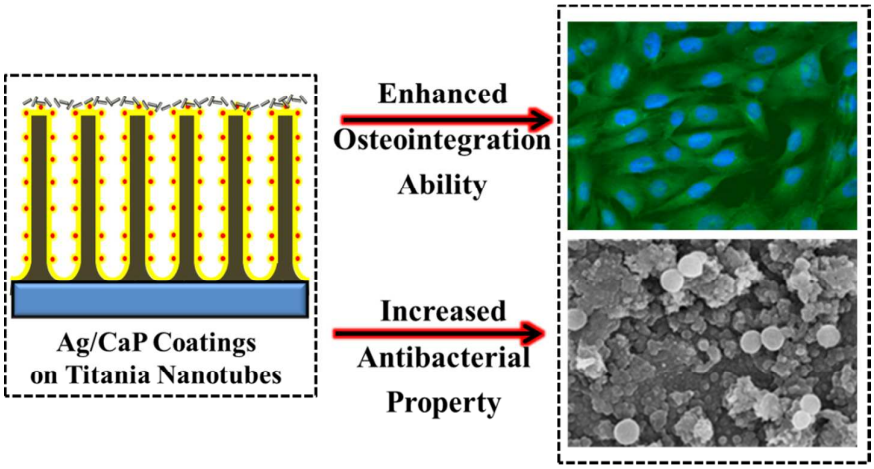

A mussel-inspired novel nano silver / calcium phosphate (CaP) composite coating was prepared on the anodized Ti, with its surface maintaining preferable biological performance and possessing long-term antibacterial ability.